A Complete Catalogue of High-Speed Solar Wind Streams during Solar Cycle 23

G. Xystouris, E. Sigala & H. Mavromichalaki

Solar Physics
A Journal for Solar and Solar-Stellar Research and the Study of Solar Terrestrial Physics

ISSN 0038-0938
Volume 289
Number 3

Sol Phys (2014) 289:995-1012
DOI 10.1007/s11207-013-0355-z

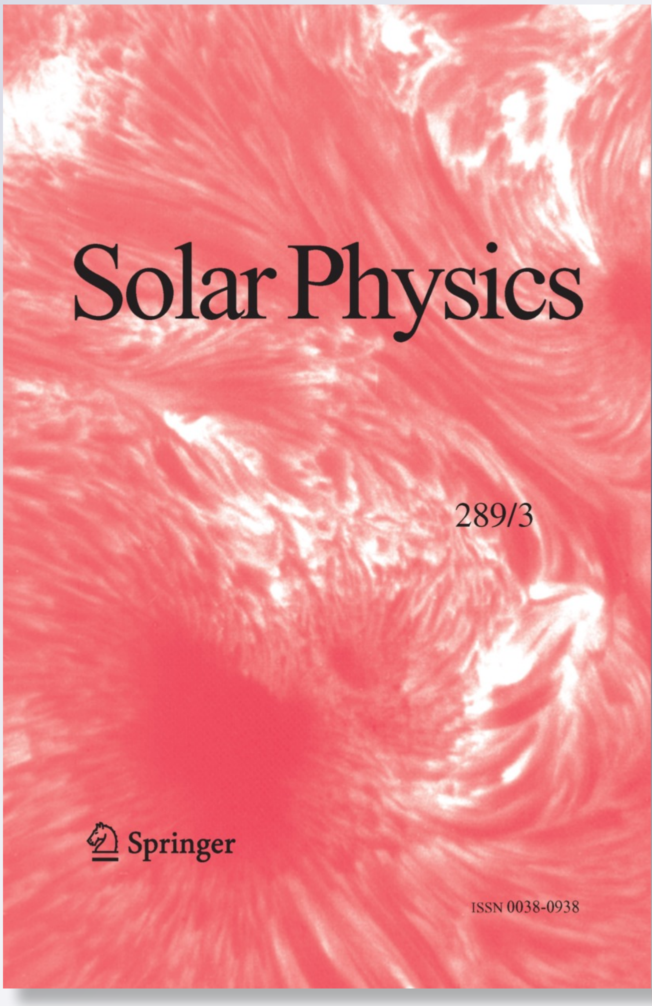

Solar Phys (2014) 289:995–1012
DOI 10.1007/s11207-013-0355-z

A Complete Catalogue of High-Speed Solar Wind Streams during Solar Cycle 23

G. Xystouris · E. Sigala · H. Mavromichalaki

Received: 19 January 2013 / Accepted: 22 June 2013 / Published online: 26 July 2013

Abstract High-speed solar wind streams (HSSWSs) are ejected from the Sun and travel into the interplanetary space. Because of their high speed, they carry out energetic particles such as protons and heavy ions, which leads to an increase in the mean interplanetary magnetic field (IMF). Since the Earth is in the path of those streams, Earth's magnetosphere interacts with the disturbed magnetic field, leading to a significant radiation-induced degradation of technological systems. These interactions provide an enhanced energy transfer from the solar wind/IMF system into the Earth's magnetosphere and initiate geomagnetic disturbances that may have a possible impact on human health. Solar cycle 23 was a particularly unusual cycle with many energetic phenomena during its descending phase and also had an extended minimum. We have identified and catalogued the HSSWSs of this cycle and determined their characteristics, such as their maximum velocity, beginning and ending time, duration, and possible sources. We identified 710 HSSWSs and compared them with the corresponding characteristics of the streams of previous solar cycles. For first time, we used the CME data to study the stream sources, which led to useful results for the monitoring and forecasting of space weather effects.

Keywords Coronal holes · Coronal mass ejections · High speed solar wind streams · Solar flares

Electronic supplementary material The online version of this article (doi:10.1007/s11207-013-0355-z) contains supplementary material, which is available to authorized users.

G. Xystouris · E. Sigala · H. Mavromichalaki (✉)
Nuclear and Particle Physics Section, Physics Department, National and Kapodistrian University of Athens, Zografos, 15784 Athens, Greece
e-mail: emavromi@phys.uoa.gr

G. Xystouris
e-mail: xystouris_geo@hotmail.com

E. Sigala
e-mail: evang.sigala@gmail.com

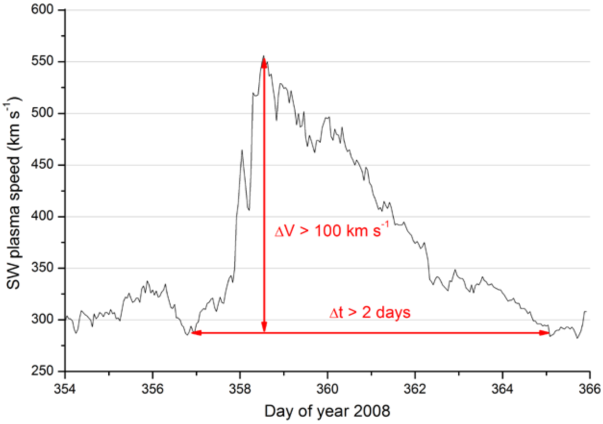

Figure 1 An example of an HSSWS. The speed difference is more than 100 km s^{-1}, the recovery time to its initial speed is longer than two days.

1. Introduction

One of the most important solar terrestrial phenomena is the near-Earth solar wind flow. It is known that this flow is connected with a wide range of phenomena and effects that become perceptible not only in space, but also on Earth, for instance as space weather, reduction in the distance to the magnetopause, geomagnetic storms, aurorae, solar radiation storms, and radio blackouts. The solar wind is a continuous flow with an average speed of 250 – 400 km s^{-1} (Parker, 1959) that tends to be organized into a stream structure (Iucci *et al.*, 1979). When a stream is generated with a flow speed faster than 400 km s^{-1}, its velocity is greater than the local velocity of the solar wind. Hence, a tangential discontinuity to the solar wind flow or a shock wave is created. In that way high-speed solar wind streams (HSSWSs) are created.

Through the years many definitions have been proposed for these events. According to Bame *et al.* (1976) and Gosling *et al.* (1976), an HSSWS is an observed variation of solar wind speed, with an increase of at least 150 km s^{-1} within a five-day interval. Intriligator (1977) described it as a rapid increase of the solar wind stream with a peak speed faster than 450 km s^{-1}. Broussard *et al.* (1978) described it as a period in which the solar wind speed is faster than 500 km s^{-1} averaged over a day. Later, Lindblad and Lundstedt (1981) defined it as a period in which the velocity difference between the lowest 3-h velocity value and the highest 3-h value of the following day is greater than 100 km s^{-1} and it lasts for at least two days. Finally, according to Mavromichalaki, Vassilaki, and Marmatsouri (1988) and Mavromichalaki and Vassilaki (1998), an HSSWS is defined as the period in which the difference between the highest speed and the mean plasma speed immediately preceding and following the stream is greater than 100 km s^{-1} in a period lasting for at least two days. This definition is used in this work because it is more appropriate for solar-terrestrial studies and so that it is the same as in our previous studies. A typical example of an HSSWS is shown in Figure 1.

The HSSWSs are produced either by corotating coronal holes or by solar flare activity. A corotating coronal hole is a low-temperature and low-density area in the Sun's atmosphere. As the Sun rotates, coronal holes pass across the Sun–Earth line; as HSSWSs are emitted from the Sun, they catch up with the previously emitted solar wind. In that way, they form a compressed interface in the interplanetary medium called a corotating interaction region (Morley, Rouillard, and Freeman, 2009). The physical features of the corotating streams, according to Mavromichalaki and Vassilaki (1998), are the following:

- The strength (B) of the interplanetary magnetic field (IMF) is proportional to the bulk speed of the stream and the polarity is constant throughout the stream, except for some fluctuations lasting a few hours.
- The proton density (n) rises to unusually high values near the leading edges of the streams.
- The proton temperature (T) varies in the same way as the flow speed.

Until recently, the HSSWSs that come from a blast wave were connected only with the flare activity. Today, owing to the development of technology for the solar observations, HSSWSs can be connected not only with flares, but also with coronal mass ejections (CMEs). In that process the material ejected by the flares compresses the plasma of the slower moving solar wind ahead of the stream and the field lines because of its expansion, causing a segregation surface with different thermodynamical and chemical properties on each side at the leading edge of the slower moving surrounding plasma (Hollweg, 1974). This structure is prevented from breaking apart by its high electrical conductivity. At the point where the emitted solar wind plasma obtains a velocity greater than the local Alfvén velocity, the shock wave is created. Finally, as in the case of the coronal hole, an HSSWS is created. The behavior of interplanetary parameters of the flare-generated streams tend to be irregular. Generally, they show the following characteristics:

- All the interplanetary parameters show simultaneous increases. Particularly, the bulk speed (V), the proton density (n), and the magnetic field strength (B) show large fluctuations during the period of the highest speed. This probably indicates fast shocks that are emitted radially.
- During the period of the highest speed, the field polarity shows inversions lasting for 3 – 4 h.
- The proton temperature does not vary simultaneously with the flow speed; instead, it tends to divert from the behavior of the flow speed, in contrast to the corotating streams.

The main reason for studying HSSWSs is that they are a potential hazard for the Earth. They contain very energetic particles, which are the source of the particle radiation dose. We can divide the dangerous areas into the geospace, the Earth atmosphere, and the ground. The hazards in the geospace are on the satellites – and technological instruments in general – and the astronauts. The hazards in the Earth atmosphere and on the ground are on the technological instruments and also on humans. The greatest danger for humans is anticipated for the aircraft passengers, due to the thinner atmospheric layer above them (for blocking the energetic particles). However, studies showed that the hazardous interaction can take place on the ground as well.

We compiled a complete catalogue of HSSWSs for solar cycle 23, from May 1996 to December 2008. In this catalogue, the characteristics of a total number of 710 well-defined HSSWSs are given, and they are classified into four different categories according to their specific parameters, such as the total annual number of HSSWSs, their sources and duration. A comparison with the corresponding characteristics of the streams of previous solar cycles was carried out.

2. Definition and Classification of HSSWSs

We used the definition for HSSWSs described in Lindblad and Lundstedt (1981) and Mavromichalaki, Vassilaki, and Marmatsouri (1988). The features that were taken into account to determine an HSSWS are the duration of the ascending and descending phases of the stream, the number of peaks that appear in the maximum phase and the existence – or

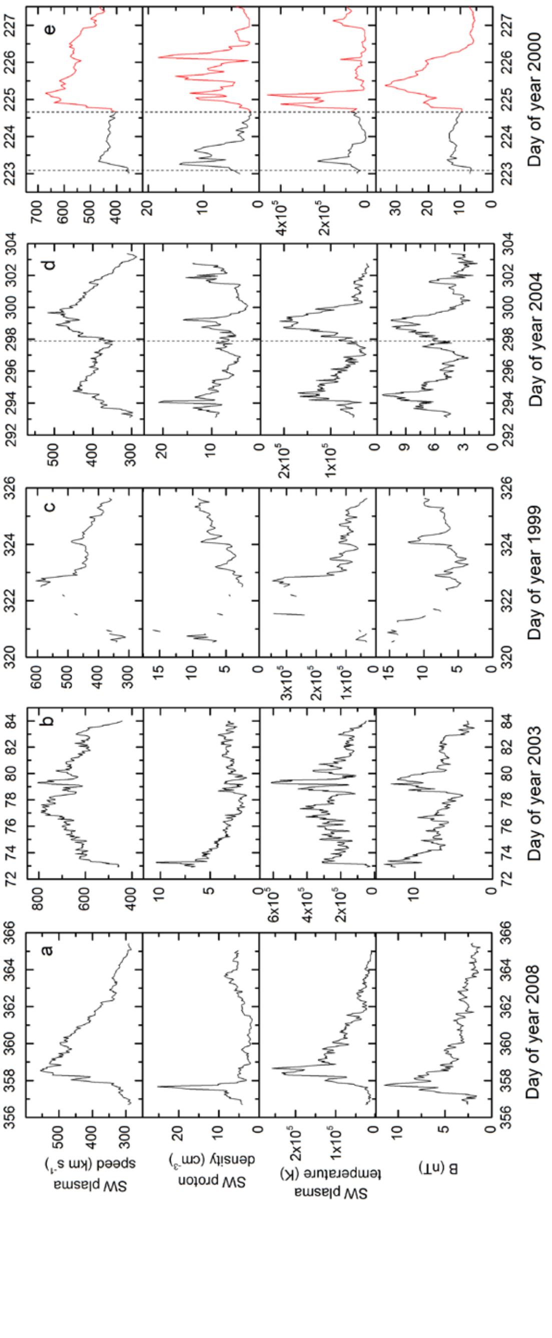

Figure 2 Categories of HSSWSs: (a) simple HSSWS, (b) HSSWS with multiple peaks, (c) HSSWS with data gaps, (d) consecutive HSSWSs, and (e) interrupted HSSWS (in black).

not – of data gaps. An HSSWS can have more than one characterization. We here used the following categories of HSSWSs, which are also illustrated in Figure 2:

- Simple HSSWSs (S): A simple HSSWS has a single peak and there is no other HSSWS present for at least 3 h before the beginning and after the end of the HSSWS (Figure 2a).
- Multiple-peak HSSWSs (M): A multi-peak HSSWS has more than one peak, and each peak is closer than one day to the following one (Figure 2b).
- HSSWS with data gap (D): When a data gap appears in any part of the HSSWS, it is characterized as an HSSWS with data gap (Figure 2c). Depending on where the data gap appears, the following approximations are adopted:
  - If there is a data gap at the beginning of the HSSWS and the stream begins from a velocity greater than 400 $\mathrm{km\,s^{-1}}$, the mean plasma velocity (V_0) for the pre-ascending phase is defined as the first good velocity data point. Its duration also begins from that point and the mean plasma velocity (V_0) that follows the stream is set at 300 – 350 $\mathrm{km\,s^{-1}}$.
  - If the data gap appears at the peak of the stream and the highest velocity ($V_{\max}$) is not visible, then $V_{\max}$ is defined as the highest velocity of the good data that appear. Therefore, according to the definition of an HSSWS, if $V_{\max}$ is 100 $\mathrm{km\,s^{-1}}$ or larger during a period of at least two days, it is registered as an HSSWS.
  - If there is a data gap in the descending phase of the stream and the plasma velocity has not reached the pre-ascending phase velocity (V_0), the last good velocity point is defined as the end of the stream. Therefore, according to the definition of an HSSWS, it is registered as an HSSWS if $V_{\max}$ is 100 $\mathrm{km\,s^{-1}}$ or larger during a period of at least two days.

In addition, the cases of consecutive HSSWSs can be determined as follows:

- If a new HSSWS appears within less than 3 h of the end of a previous one, we call this a consecutive HSSWS (Figure 2d). For groups with more than two HSSWSs, we count a case of consecutive HSSWSs for every two consecutive HSSWSs, *e.g.* for a group of four HSSWSs, we have a case of three consecutive HSSWSs.

Finally, the most important feature added in this work is the addition of a special category of HSSWSs, called interrupted HSSWSs.

- Interrupted HSSWSs: An interruption in an HSSWS is described as a new HSSWS in an on-going one (Figure 2e). Based on the definition of HSSWSs, this is characterized by two phases: an ascending and a descending phase. The ascending phase is defined as the period from the beginning of the HSSWS to the moment that the HSSWS reaches its highest velocity. The descending phase is defined as the period of the moment that the HSSWS has reached its highest velocity until the end of the HSSWS. Therefore, the interruption may take place either in the ascending or in the descending phase. Based on that, we categorize them into two subcategories:
  - Interrupted HSSWSs in the ascending phase: These HSSWSs appear at the end of the descending phase of an ongoing HSSWS. Before the velocity of the first HSSWS reaches the mean value of the pre-ascending phase, it may rise again due to the incoming solar wind shock. That point defines the preceding V_0 of the interrupted stream. The end of the interrupted HSSWS is defined when the plasma velocity decreases to 330 $\mathrm{km\,s^{-1}}$ and its duration can be defined accordingly. If $V_{\max}$ exceeds the value of V_0 preceding the stream by 100 $\mathrm{km\,s^{-1}}$ or more and its duration is shorter than two days, the second stream is defined as an interrupted HSSWS.

– Interrupted HSSWSs in the descending phase: These HSSWSs begin as a simple HSSWS, but the interruption occurs in its descending phase, before the plasma velocity reaches the pre-ascending phase velocity, V_0. The end of the stream is defined as the point of the interruption and its duration can be defined accordingly. If V_{max} exceeds the value of V_0 preceding the stream by 100 km s^{-1} or more and its duration is shorter than two days, the stream is defined as an interrupted HSSWS.

3. Data Selection and Analysis

We used solar and interplanetary data obtained from the OMNI database (http://omniweb.gsfc.nasa.gov/ow.html). The following parameters were taken into account: the Bartels rotation number, the solar wind flow speed, the solar wind proton temperature, the solar wind magnetic field strength, and the solar wind proton density for the time period from May 1996 until December 2008. The IMF data were selected from the National Space Science Data Center database (http://omniweb.gsfc.nasa.gov/html/polarity/polarity.html).

The examined time period is from May 1996 until December 2008 and covers solar cycle 23 according to the Marshall Space Flight Center database (http://solarscience.msfc.nasa.gov). This period was divided into four phases based on the solar activity level:

i) Ascending phase, from May 1996 until April 1999,
ii) Maximum phase, from May 1999 until December 2002,
iii) Descending phase, from January 2003 until December 2006,
iv) Minimum phase, from January 2007 until December 2008.

According to our criteria, the HSSWSs in Solar Cycle 23 were determined and a total number of 710 HSSWSs were identified. A catalogue with all these HSSWSs and their parameters was compiled and is provided as electronic supplementary material (Table 1). The first column shows the number of HSSWS (the asterisk denotes the interrupted HSSWS). The second column shows the exact start time of the HSSWS and the third column gives the Bartels rotation number and day. The fourth column gives the IMF polarity during the examined HSSWS. The fifth column shows the date of the highest solar wind speed. The sixth column gives the mean solar wind speed, while the seventh column shows the highest speed of the stream. The eighth column shows the HSSWS duration. The ninth column denotes the HSSWS category (S for simple HSSWS, M for HSSWS with multiple peaks, and D for HSSWS with data gaps) and the tenth column gives the source of the HSSWS, where CH is a stream originating from a coronal hole, F is a flare-generated stream, CME is an HSSWS originating from a CME, and the question mark denotes that a source for this HSSWS could not be found.

The distribution of the total number (T) as well as the number of various categories of HSSWSs in each phase of solar cycle 23 is given in Table 2. The second column denotes the number of simple HSSWSs (S), the third one denotes the number of HSSWSs with multiple peaks (M), the fourth denotes the number of HSSWSs with data gaps (D), and the fifth denotes the number of HSSWSs with multiple peaks and data gaps (DM). The last column denotes the ratio of the consecutive cases of HSSWSs to the total number of them (C/T). The largest ratio of consecutive cases to the total number of HSSWSs appears in the maximum phase of solar cycle 23 (71 %) followed closely by the descending phase (68 %). This shows that in both phases the generation rate of HSSWSs is very high, unlike in the ascending and minimum phases, where the generation rate is lower.

It is noteworthy that an analogous catalogue on HSSWSs during solar cycle 23 was also presented by Gupta and Badruddin (2010). This catalogue covered the time period of 1996

Table 2 Distributions of HSSWSs according to the categories in each phase of solar cycle 23. The ratio of the consecutive cases to the total number of HSSWSs for each phase of solar cycle 23 is also given.

Solar cycle phase	Total HSSWSs (T)	Simple HSSWSs (S)	Multiple peak HSSWS (M)	HSSWSs with data gaps (D)	HSSWSs with multiple peaks and data gaps (D & M)	Consecutive HSSWSs (C)	Ratio consecutive to total HSSWSs (C/T)
Ascending phase	153	87	53	12	1	52	0.34
Maximum phase	214	60	150	3	1	151	0.71
Descending phase	239	75	157	2	5	162	0.68
Minimum phase	104	75	29	0	0	29	0.28

to 2007 and presented 465 cases of HSSWWs. Our catalogue covers the full time period of solar cycle 23, and we identified 710 HSSWSs. This difference is due to the process of identifying and cataloguing each stream. We tried to relate each HSSWS to a single possible source (solar flares, coronal mass ejections, or coronal holes), while Gupta and Badruddin (2010) did not separate multiple sources of the streams. As a result, five different types of streams were determined and identified in this catalogue, as described in detail in Section 2 and presented in Figure 2. Moreover, only coronal holes, CMEs, and shock waves were considered as the main sources by Gupta and Badruddin (2010), excluding solar flares as even possible sources. These are some of the reasons for proposing this new, more detailed catalogue.

4. Characteristics of HSSWSs

4.1. Total Number of HSSWSs

The yearly distribution of the total number of the HSSWSs is given in Figure 3a. It is interesting to note that the year 2003 contains the largest number of HSSWSs throughout solar cycle 23, with approximately six HSSWSs per month. This year was characterized by many extreme solar events, such as those on 28 and 29 October 2003 and on 4 and 20 November 2003 (Belov *et al.*, 2005). In addition, most of the HSSWSs occurred during the descending phase with a percentage of 34 % of the total number of HSSWSs of this cycle, as is illustrated in Figure 3b. Then the ascending phase and the maximum phase follow, with percentages of 22 % and 30 %, respectively. During the minimum phase, the number of HSSWS is lowest with a percentage of only 15 % of the total number of HSSWSs. These results agree with the corresponding results of the previous cycles 20, 21, and 22. Maris and Maris (2005) concluded that during solar cycles 20–22 the occurrence rate of the streams was higher during the descending and minimum phases, regardless of their solar sources (coronal holes/solar flares).

4.2. Duration of HSSWSs

It is known that there are many differences between odd- and even-numbered solar cycles. The odd cycles, as the examined cycle 23, appear to be more active than the even ones

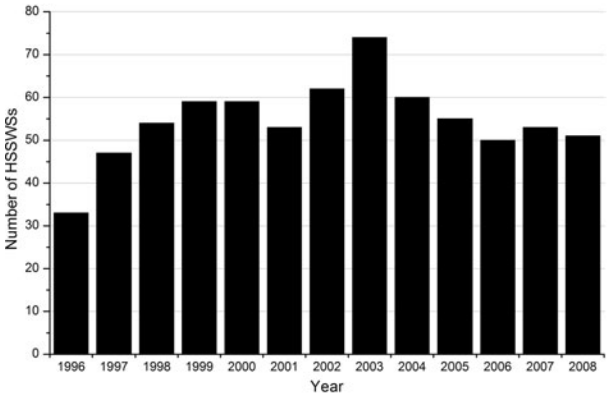

Figure 3a Annual number of HSSWSs for solar cycle 23 (from May 1996 to December 2008).

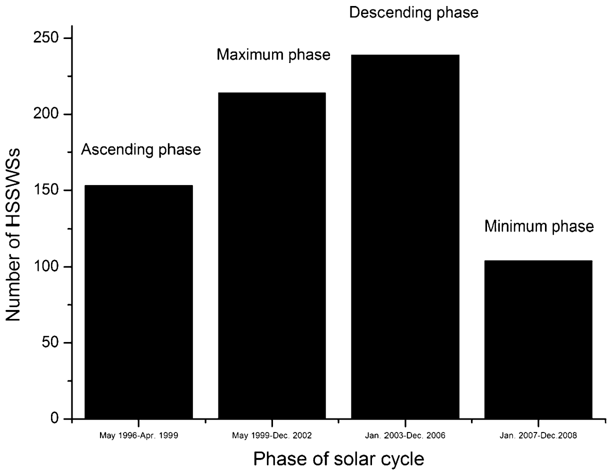

Figure 3b Total number of HSSWSs in each phase of solar cycle 23.

(Mavromichalaki and Vassilaki, 1998). Previous studies of solar cycles 20, 21, and 22 have shown that the distribution of the HSSWSs shows a maximum around 4 – 6 days for the even cycles and almost 6 – 8 days for the odd ones (Maris and Maris, 2005). Gupta and Badruddin (2010) divided the streams of solar cycle 23 into three categories, namely: i) short-duration high-speed streams (HSS) with $\Delta t \leq 4$ days, ii) medium-duration HSS with 4 days $< \Delta t \leq$ 8 days, and iii) long-duration HSS with $\Delta t \geq 8$ days with percentages of 12 %, 46 %, and 43 % out of total 465 high-speed streams observed. Additionally, they observed that short-duration HSS are more frequent in the ascending phase, there are fewer medium-duration HSS in the declining phase, and the long-duration HSS prevail during the maximum and declining phases of solar cycle 23.

We divided the HSSWSs into the following bins according to their duration (see also Figure 4a):

i) shorter than two days (they are symbolized as "2−" days),
ii) between two and four days,
iii) between four and six days,
iv) between six and eight days,
v) between eight and ten days,
vi) ten days or longer, symbolized as "10+" days.

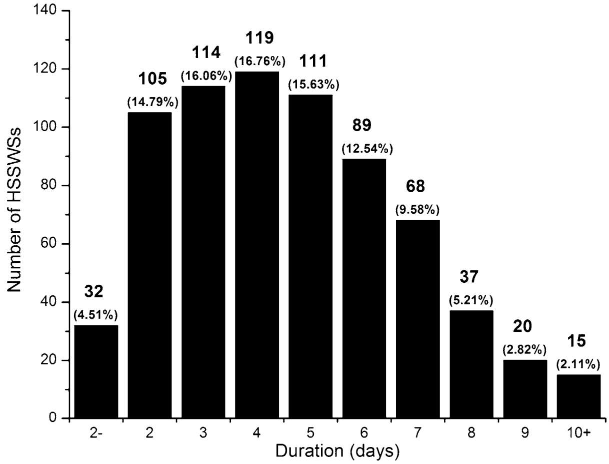

Figure 4a Distribution of the HSSWS duration during solar cycle 23.

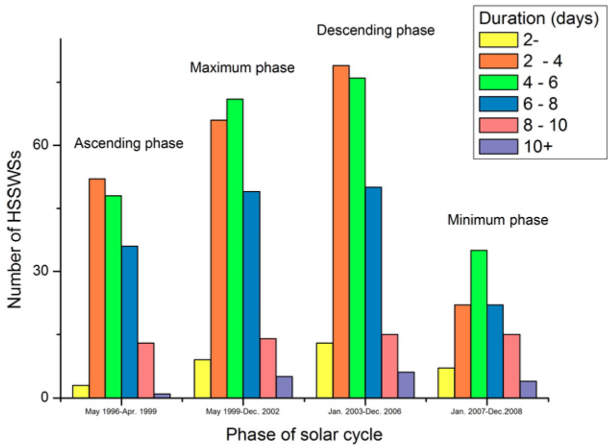

Figure 4b Distribution of the HSSWS duration during different phases of solar cycle 23.

This division revealed that the prevalent HSSWSs are those whose duration ranges between four and six days with a percentage of 32.4 % out of 710 HSSWSs observed. In a decreasing order, the HSSWSs appear with durations between two-four days and six-eight days with percentages of 31 % and 22 %, respectively. The least frequent HSSWSs are those symbolized as 2− and 10+, which constitute only 4 % and 2 % out of the total 710 HSSWSs, respectively. Therefore, taking into account the statistical error for each duration bin, apparently most of the HSSWSs in solar cycle 23 lasted from three to six days (Table 3a). This conclusion agrees with the previous study of Gupta and Badruddin (2010), where the prevalent HSSWS are those characterized as medium-duration high-speed streams with a duration of four days $< \Delta t \leq 8$ days (46 %).

Regarding the distribution of HSSWS duration in terms of the phases of the solar cycle, as seen in Figure 4b and in Table 3b, most of the HSSWSs of the ascending phase have a duration between two and four days (34 % out of the total 153 HSSWSs in the ascending phase). In the maximum phase the HSSWSs that last between four and six days (33 % of 214 HSSWSs in the maximum phase) are prevalent. Additionally, during the descending phase the HSSWSs that last from two to four days (33 % of the 239 observed HSSWSs for

Table 3a Yearly number of HSSWSs according to their duration.

Year	Number of streams according to their duration					
	2− days	2 – 4 days	4 – 6 days	6 – 8 days	8 – 10 days	10+ days
1996	1	7	16	6	2	1
1997	0	15	14	15	3	0
1998	1	21	14	11	7	0
1999	2	20	20	12	3	2
2000	7	20	16	12	3	1
2001	0	12	20	14	5	2
2002	1	23	19	15	4	0
2003	7	28	23	12	2	2
2004	2	24	18	10	4	2
2005	3	13	19	13	6	1
2006	1	14	16	15	3	1
2007	2	9	20	16	3	3
2008	5	13	15	6	12	0
Total	32	219	230	157	57	15

Table 3b Number of streams according to their duration in each phase of solar cycle 23.

Solar cycle phase	Number of streams according to their duration					
	2− days	2 – 4 days	4 – 6 days	6 – 8 days	8 – 10 days	10+ days
Ascending (May 1996 – Apr. 1999)	3	52	48	36	13	1
Maximum (May 1999 – Dec. 2002)	9	66	71	49	14	5
Descending (Jan. 2003 – Dec. 2006)	13	79	76	50	15	6
Minimum (Jan. 2007 – Dec. 2008)	7	22	35	22	15	3
Total	32	219	230	157	57	15

the descending phase) are most frequent, followed closely by the HSSWSs that last from four to six days (32 % of the 239 observed HSSWSs). Finally, the most frequently observed HSSWSs during the minimum phase are those with a duration between four and six days (34 % out 104 HHSWSs during minimum). It is worth mentioning that the most frequent interrupted HSSWS (symbolized as 2− days) are observed during the descending phase with a percentage of 41 % of the total number of them, as a result of high solar activity during that phase, when HSSWSs were constantly generated, which left no space for the interrupted HSSWSs to emerge as a normal HSSWS. The HSSWSs characterized as 10+ days also appear most frequently during the descending phase, more specifically, 40 % of the total 15 HSSWSs in the 10+ days group. Finally, it is important to mention that the HSSWS with the longest duration of 16.71 days was observed during the maximum phase.

4.3. Maximum Speed of HSSWSs

To derive the distribution of the highest speeds, 710 HSSWSs were divided into bins of 100 km s^{-1}, from 400 km s^{-1} to 1199 km s^{-1} in each of the four phases of solar cycle 23.

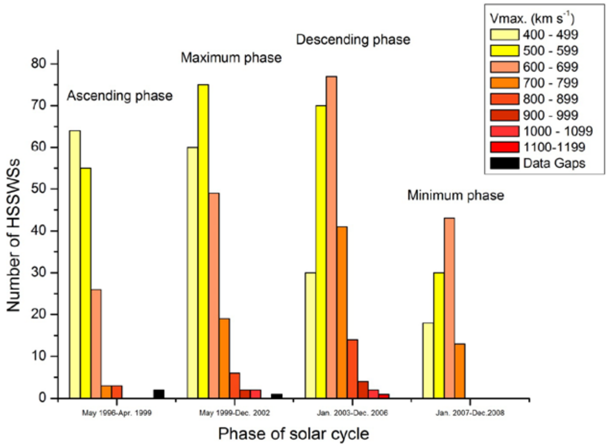

Figure 5 Distribution of $V_{\max}$ in each phase of solar cycle 23.

The streams with data gaps in $V_{\max}$ were also taken into consideration. Figure 5 presents an overview taking into account the phases of the solar cycle according to this study, which shows that in the ascending phase most of the HSSWSs are observed to have $V_{\max}$ between 400 km s^{-1} and 499 km s^{-1} (almost 42 % of 153 HSSWS in the ascending phase). In the maximum phase, $V_{\max}$ increases to 500 – 599 km s^{-1} (35 % of 214 HSSWSs in the maximum phase). Then, in the descending phase $V_{\max}$ continues to rise; 29 % of the 239 descending phase HSSWSs have $V_{\max}$ between 500 km s^{-1} and 599 km s^{-1}, but 32 % of them also have $V_{\max}$ between 600 and 699 km s^{-1}. Finally, in the minimum phase most of the HSSWSs (41 % of 104 streams) have $V_{\max}$ of 600 – 699 km s^{-1}.

Furthermore, in the ascending phase the highest number of HSSWSs has $V_{\max}$ of 400 – 499 km s^{-1}, followed by the 500 – 599 km s^{-1} bin (36 %) and the 600 – 699 km s^{-1} bin (17 %). The amount of 2 % of HSSWSs in the ascending phase belongs to the bins of 700 – 799 km s^{-1} and 800 – 899 km s^{-1}. Moreover, there was no HSSWS observed with $V_{\max}$ up to 900 km s^{-1}, while two HSSWSs had data gaps in their $V_{\max}$.

In the maximum phase, the number of HSSWSs in the bin of 400 – 499 km s^{-1} starts to decrease (28 % out of 214 HSSWSs) and the predominant bin is that of 500 – 599 km s^{-1} (35 %), followed by the 600 – 699 km s^{-1} bin (23 %), the 700 – 799 km s^{-1} bin (9 %), and the 800 – 899 km s^{-1} bin (3 %). It is worth mentioning that two HSSWSs are observed with $V_{\max}$ in the 900 – 999 km s^{-1} bin and also in the 1000 – 1099 km s^{-1} bin (1 % respectively). Only one HSSWS had a data gap in $V_{\max}$.

Subsequently, during the descending phase the number of HSSWSs belonging to the 500 – 599 km s^{-1} bin is lower than the number of HSSWSs belonging to the 600 – 699 km s^{-1} bin. In this phase, only 13 % of the HSSWSs belong to the 400 – 499 km s^{-1} bin, while 17 %, 6 %, and 2 % of the 239 descending phase HSSWSs constitute the 700 – 799 km s^{-1} bin, the 800 – 899 km s^{-1} bin, and the 900 – 999 km s^{-1} bin, respectively. The HSSWSs with higher $V_{\max}$ are also observed more frequently, as four of the 239 HSSWSs had $V_{\max}$ between 900 km s^{-1} and 999 km s^{-1} and two HSSWSs had $V_{\max}$ between 1000 km s^{-1} and 1099 km s^{-1}. Finally, in this phase, the HSSWS with the highest $V_{\max}$ of this cycle was observed, reaching a speed of 1189 km s^{-1}.

Finally, in the minimum phase, most of the HSSWSs belong to the 600 – 699 km s^{-1} bin, followed by the 500 – 599 km s^{-1} bin (29 %), 400 – 499 km s^{-1} bin (almost 17 %), and 700 – 799 km s^{-1} bin (13 %). It is worth mentioning that only one HSSWS had $V_{\max}$ between

Table 4a Yearly number of HSSWSs according to their highest speed.

Year	Number of streams according to their V_{max}								
	400 – 499 [km s^{-1}]	500 – 599 [km s^{-1}]	600 – 699 [km s^{-1}]	700 – 799 [km s^{-1}]	800 – 899 [km s^{-1}]	900 – 999 [km s^{-1}]	1000 – 1099 [km s^{-1}]	1100 – 1199 [km s^{-1}]	Data gaps
1996	11	14	8	0	0	0	0	0	0
1997	27	14	3	1	0	0	0	0	2
1998	23	15	11	2	3	0	0	0	0
1999	14	21	19	4	1	0	0	0	0
2000	20	17	14	4	2	1	1	0	0
2001	12	24	9	4	2	0	1	0	1
2002	17	25	11	7	1	1	0	0	0
2003	4	18	23	19	9	0	0	1	0
2004	9	26	17	5	2	0	1	0	0
2005	6	12	17	13	2	4	1	0	0
2006	11	14	20	4	1	0	0	0	0
2007	9	14	27	3	0	0	0	0	0
2008	9	16	16	10	0	0	0	0	0
Total	172	230	195	76	23	6	4	1	3

800 km s^{-1} and 899 km s^{-1}. During the descending and minimum phases there was no data gap in V_{max} of any HSSWS.

In conclusion, the peak of the V_{max} distribution continues to rise until the descending phase, when it reaches values of 600 – 699 km s^{-1}. Then instead of dropping in the minimum, it remains at the same values. In addition, it is important to mention that the highest values of the observed V_{max} are 922 km s^{-1} (in 2002), 1010 km s^{-1} (in 2000), 1027 km s^{-1} (in 2004), 1040 km s^{-1} (in 2001), 1059 km s^{-1} (in 2005), and 1189 km s^{-1} (in 2003). The yearly distribution and the distribution over the solar cycle phases of the highest speed of HSSWSs are given in Tables 4a and 4b.

4.4. Sources of HSSWSs

Possible sources of HSSWSs are the coronal holes and the solar flares, which are classified into corotating and flare-generated streams, respectively. Lindblad and Lundstedt (1981, 1983) and Lindblad, Lundstedt, and Larsson (1989) presented the HSSWSs observed by near-Earth spacecraft in the periods of 1964 – 1975, 1975 – 1978, and 1978 – 1982 (solar cycles 20 and partly 21). Mavromichalaki, Vassilaki, and Marmatsouri (1988) presented a catalogue of HSSWSs for the period of 1972 – 1984. As a continuation of the previously published catalogue, Mavromichalaki and Vassilaki (1998) presented the HSSWS catalogue for the period of 1985 – 1996 (cycle 22) and classified them into the above mentioned categories. The conclusions of this last paper indicate that the number of flare-generated streams is larger around the solar maximum (1969, 1979, and 1989 of cycles 20, 21, and 22, respectively), while corotating streams are more frequent around the solar minimum. Maris and Maris (2005) also followed this classification of HSSWSs for solar cycles 20 – 22 and studied the streams produced by coronal holes (CH_HSPS) and those produced by solar flares (FG_HSPS). They revealed that CH_HSPS prevail during the minimum phases of solar cycles because large coronal holes extend towards the equator in the minimum phases of solar cycles, while the variation of FG_HSPS follows the 11-year cycle of sunspots.

Table 4b Number of streams with different $V_{\max}$ in each phase of solar cycle 23.

Phase of solar cycle 23	Number of streams according to their $V_{\max}$								
	400 – 499 [$\mathrm{km\,s^{-1}}$]	500 – 599 [$\mathrm{km\,s^{-1}}$]	600 – 699 [$\mathrm{km\,s^{-1}}$]	700 – 799 [$\mathrm{km\,s^{-1}}$]	800 – 899 [$\mathrm{km\,s^{-1}}$]	900 – 999 [$\mathrm{km\,s^{-1}}$]	1000 – 1099 [$\mathrm{km\,s^{-1}}$]	1100 – 1199 [$\mathrm{km\,s^{-1}}$]	Data gaps
Ascending phase (May 1996 – Apr. 1999)	64	55	26	3	3	0	0	0	2
Maximum phase (May 1999 – Dec. 2002)	60	75	49	19	6	2	2	0	1
Descending phase (Jan. 2003 – Dec. 2006)	30	70	77	41	14	4	2	1	0
Minimum phase (Jan. 2007 – Dec. 2008)	18	30	43	13	0	0	0	0	0
Total	172	230	195	76	23	6	4	1	3

Furthermore, Mavromichalaki and Vassilaki (1998) concluded that the activity of solar cycle 21, which is an odd cycle, was higher than the activity of solar cycles 20 and 22, which are even cycles. This reveals a periodicity that is correlated with the 22-year variation of solar magnetic field (Legrand and Simon, 1981; Simon and Legrand, 1992; Mavromichalaki, Vassilaki, and Tsagouri, 1997; Mavromichalaki and Vassilaki, 1998). It also indicates different behaviors between odd and even cycles, such as the large number of flare-generated streams during the odd cycles and the appearance of two maxima during the even cycles. Maris and Maris (2005) showed that solar cycles 20 and 22 have similar dynamics of the FG_HSPS and CH_HSPS parameters during the maximum, descending, and reversal intervals. They revealed that the dominance of solar cycle 21 in all the CH_HSPS parameters against solar cycles 20 and 22 in almost all the phases could be due to the same structure of the Hale cycle, though solar cycle 21 has a larger number of FG_HSPS than the even cycles.

In addition, it is worth mentioning that the corotating streams are connected with simple decreases of cosmic rays recorded at ground-based stations and the flare-generated streams produce Forbush decreases on Earth (Iucci *et al.*, 1979; Mavromichalaki, Vassilaki, and Marmatsouri, 1988). Moreover, strong flares recorded by neutron monitors on Earth produced strong ground-level enhancements (GLE) associated with energetic solar proton events, such as those of the solar cycle 22 (Belov and Eroshenko, 1996).

Recently, Gupta and Badruddin (2010) divided the HSSWSs of solar cycle 23 into five groups, namely, those associated with i) a single coronal hole (SCH), ii) a single mass ejection (SME), iii) multiple coronal holes (MCH), iv) multiple mass ejections (MME), and v) compound streams associated with both coronal hole(s) and mass ejection(s) (CMP). These authors concluded that the majority of the total 465 identified streams (43 %) are produced by a single coronal hole, followed by the compound streams (26 %), the streams produced by multiple coronal holes (18 %), and a single mass ejection (9 %). The minority of them (4 %) are related to multiple mass ejections.

Table 5a Yearly number of HSSWSs according to their sources.

Year	Number of streams with different sources					
	CH	F	CME	F/CME	F/CME(?)	?
1996	28	1	0	0	0	4
1997	27	16	1	3	0	1
1998	25	23	0	6	1	0
1999	45	9	0	4	1	0
2000	27	29	0	2	1	0
2001	21	19	0	11	1	0
2002	38	17	0	5	1	0
2003	56	15	0	2	1	0
2004	40	15	0	4	1	0
2005	35	14	0	6	0	0
2006	42	6	0	1	1	0
2007	48	3	0	0	0	2
2008	40	7	1	0	0	3
Total	472	174	2	44	8	10

As a continuation of the previous works of Mavromichalaki, Vassilaki, and Marmatsouri (1988) and Mavromichalaki and Vassilaki (1998), the HSSWSs are here classified as follows: corotating streams (CH) that are produced by coronal holes, and flare-generated streams (F) that are associated with active regions producing flares. For this solar cycle good quality coronagraph data are available, therefore we attempted to take CMEs into account as a possible source of HSSWSs. Therefore, the total number of HSSWSs of this cycle is divided into six groups:

i) corotating streams, produced by corotating coronal holes (CH),
ii) flare-generated streams, produced only by a flare (F),
iii) CME-generated streams produced by only a CME (CME),
iv) flare-generated and CME-generated streams produced by both flare and CME (F/CME),
v) CME-generated streams produced by only a CME (CME),
vi) flare-generated and CME-generated streams when the responsible source is not clear (F/CME ?), and
(vii) streams with no clear origin (?).

In these terms, the distributions of HSSWSs per year and per phase of the solar cycle are statistically studied and are given in Tables 5a and 5b, respectively.

The annual distribution of HSSWSs on the basis of their origin, as shown in Figure 6a, reveals that most of the streams of solar cycle 23 are the corotating streams (CH). The majority of these streams (56 CH) were produced in 2003 and the minority of them (21 CH) in 2001, while the majority of streams that are related to both flares and CMEs (11 F/CME) were observed in 2001. As we show, the maximum of the distribution of flare-generated streams (29 F) took place in the year 2000. It is worth mentioning that CME-generated streams showed no notable 11-year variation. These CME HSSWSs took place in the years 1997 and 2008. The same is observed for the flare-generated and CME generated streams when the responsible source is not clear (F/CME ?); these took place in the years 1999, 2000, 2001, 2002, 2003, 2004, and 2006. Ten HSSWSs have doubtful and no clear origin (?). Compared with the total number of HSSWSs, their number presents a negligible error.

Table 5b Number of streams according to their sources in each phase of solar cycle 23 (May 1996 – December 2008).

Solar cycle phase	Number of HSSWSs	Number of streams with different sources				
		CH	F	CME	F/CME	F/CME ?
Ascending (May 1996 – Apr. 1999)	153	97	41	1	10	7
Maximum (May 1999 – Dec. 2002)	214	114	73	0	21	3
Descending (Jan. 2003 – Dec. 2006)	239	173	50	0	13	3
Minimum (Jan. 2007 – Dec. 2008)	104	88	10	1	0	5
Total	710	472	174	2	44	18

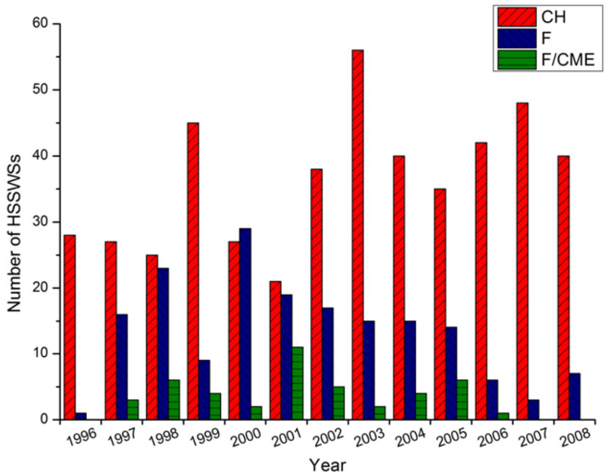

Figure 6a Annual distribution of the HSSWS sources.

Regarding the source distribution over the phases of solar cycle 23, as presented in Figure 6b, it is proved that most of the HSSWSs were produced by coronal holes. They took place in the descending and the ascending phases of the cycle, where 131 CH (40 % of total 434 CH) and 97 CH (22 %) are observed, respectively. On the other hand, the F and the F/CME HSSWSs show an 11-year variation. Most of them, in percentages of 42 % of total 174 F and 48 % of 44 F/CME HSSWS, are observed in the maximum phase, but their number is still significantly lower than the CH HSSWSs. Finally, for consistency, two CME HSSWSs were observed in the ascending and minimum phases, but this result is not significant because of its small number.

Concluding, the majority of HSSWSs of this cycle are CH HSSWSs even though solar cycle 23 is an odd-numbered cycle. This is shown in both Figures 6a and 6b, where 63 % out of total 153 HSSWSs in the ascending phase, 36 % of 214 HSSWSs in the maximum, 72 % of 239 HSSWSs in the descending phase, and 85 % of 104 HSSWSs during the minimum are CH HSSWSs. Maris and Maris (2005) arrived at the same conclusion. They mentioned that "the best-established sources of the HSPSs are the coronal holes – the regions with open magnetic fields". The majority of F HSSWSs appeared in the maximum phase (34 % of 214 HSSWS), which agrees with the previous studies that dealt with the maximum phase

Figure 6b Distribution of the HSSWS sources for each phase of solar cycle 23.

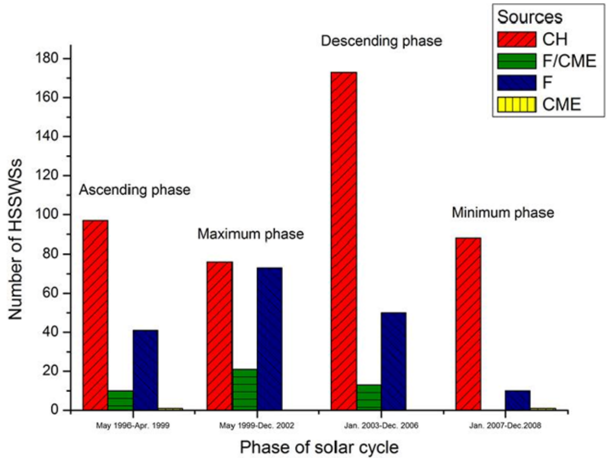

(1969, 1979, and 1989 for solar cycles 20, 21, and 22, respectively). This because the large coronal holes that exist during the solar minimum produce many corotating streams. As a final conclusion, the number of F and F/CME HSSWSs is higher around the maximum phase, showing an 11-year variation; this agrees with what was observed by plotting the number of F HSSWSs for each year for solar cycles 20 – 22 (Mavromichalaki and Vassilaki, 1998) and with the statistical study of flare-generated streams of the period of 1964 – 1996 (Maris and Maris, 2005). In contrast, the number of CH HSSWSs is high throughout the solar cycle, while according to Mavromichalaki and Vassilaki (1998) it was expected to be high only in the ascending phase and in the minimum.

5. Conclusions

A detailed analysis of the HSSWSs registered in the time interval of 1996 – 2008, which covers solar cycle 23, was carried out and 710 HSSWSs were identified. We found that 434 of them were generated by corotating coronal holes (CH), 261 events were generated by flares, CMEs, or both (F, CME, or F/CME), and the origin of 15 events was not clear. This means that more than half of them are generated by coronal holes, which was not observed in the previous cycles.

It is known that solar cycle 23 was one of the most active cycles, characterized by many extreme solar events. We found that the most frequent appearance of HSSWSs (73 HSSWSs) took place in the year 2003, in the descending phase of this cycle, immediately after the secondary maximum of the solar activity. In addition, the greatest fraction of consecutive HSSWSs appeared in both the maximum and descending phases of solar cycle 23, where seven out of ten HSSWSs were consecutive.

The average duration of the HSSWSs of solar cycle 23 according to this work is three to five days. Compared with previous works (Mavromichalaki, Vassilaki, and Marmatsouri, 1988; Mavromichalaki and Vassilaki, 1998), we noticed that the duration of HSSWSs tends to be shorter in the recent solar cycles: the average duration of the HSSWSs was six to seven days in cycle 21, four to five days in cycle 22, and three to five days in cycle 23. This might be a hint of a more active Sun as the cycle lasts, because every preceding generation of HSSWSs prevents the Sun from generating long-duration HSSWSs. At least we may claim that our results on solar cycle 23 are more reliable than the work on the previous cycles because of the availability of more advanced equipment and spacecraft for the detection of the solar wind characteristics, and because of a more complete data base.

For the highest velocity of HSSWSs we concluded that in the ascending phase most of the HSSWSs are observed to have $V_{\max}$ between 400 km s^{-1} and 499 km s^{-1}, in the maximum phase the peak of $V_{\max}$ distribution increases to 500 – 599 km s^{-1}, in the descending phase the $V_{\max}$ peak continues to rise because most of the HSSWSs have $V_{\max}$ of 500 – 599 km s^{-1} and 600 – 699 km s^{-1}. The minimum phase is dominated by HSSWSs with $V_{\max}$ of 600 – 699 km s^{-1}. It is notable that the HSSWSs with the highest values of $V_{\max}$ (900 – 999 km s^{-1}, 1000 – 1099 km s^{-1}, and 1100 – 1199 km s^{-1} bins) are observed more frequently in the maximum and the descending phases. In time evolution, it is clear that the $V_{\max}$ peak increases until the descending phase, where it stays stable to the minimum phase. In the minimum phase $V_{\max}$ higher than 800 km s^{-1} vanished.

Finally, the annual distribution of the sources of HSSWSs showed that most of the HSSWSs that occurred in solar cycle 23 are CH HSSWSs, with the maximum of their distribution in the year 2003 and the minimum in the year 2001. The majority of F/CME and F HSSWSs combined occurred in 2001, 2000, and 1998, respectively. The CME and F/CME? HSSWSs have no notable distribution because they have only very few data points, while ten HSSWSs were found with doubtful origin. Although solar cycle 23 is an odd-numbered cycle, the distributions of HSSWSs according to their sources and the phases reveal that most of the CH HSSWSs occurred during the descending and ascending phases. However, there were many CH HSSWSs throughout the whole cycle. Moreover, most of the F and F/CME HSSWSs were observed in the maximum phase, showing an 11-year variation. The conclusions of this work agree well with the studies of the solar cycles 20, 21, and 22.

In summary, we can say that one of the most dynamical interplanetary phenomena of solar-terrestrial physics is definitely the passage of solar wind streams near the Earth environment. Studies of various aspects of the solar wind velocity variability with time in the ecliptic plane revealed a tendency for the solar wind to be organised as stream structures (*e.g.* Iucci *et al.*, 1979; Lindblad and Lundstedt, 1981). In particular, the occurrence rate, characteristics, and the long-term variations of the high-speed streams for solar cycles 20, 21, and 22 have been studied in Mavromichalaki and Vassilaki (1998) and Maris and Maris (2005). Reference catalogues of high-speed solar wind streams observed near the Earth have been produced, considering two possible solar sources, coronal holes and active regions that produce flares. In this work a new high-speed stream source related to the CMEs was added because new CME data are now available. In the future, an extended study of the sources of a large number of observed events during solar cycle 23 will be very useful for space weather studies.

Acknowledgements Thanks are due to all colleagues who kindly provide all the solar and interplanetary data used in this work. We also acknowledge the Special Research Account of the National and Kapodistrian University of Athens, for supporting G. Xystouris to present this work in the Space Weather Effects on Humans Conference held in Moscow (3 – 7 June 2012). Moreover, we thank A. Hillaris for useful discussions.

References

Bame, S.J., Asbridge, J.R., Feldman, W.C., Gosling, J.T.: 1976, *Astrophys. J.* **207**, 977 – 980.
Belov, A.V., Eroshenko, E.A.: 1996, *Radiat. Meas.* **26**, 461 – 466.
Belov, A., Baisultanova, L., Eroshenko, E., Mavromichalaki, H., Yanke, V., Pchelkin, V., Plainaki, C., Mariatos, G.: 2005, *J. Geophys. Res.* **110**, A09S20.
Broussard, R.M., Tousey, R., Underwood, J.H., Sheeley, N.R. Jr.: 1978, *Solar Phys.* **56**, 161 – 183.
Gosling, J.T., Asbridge, J.R., Bame, S.J., Feldman, W.C.: 1976, *J. Geophys. Res.* **81**, 5061 – 5070.

Gupta, V., Badruddin: 2010, *Solar Phys.* **264**, 165 – 188.
Hollweg, J.V.: 1974, *Publ. Astron. Soc. Pac.* **86**, 561 – 594.
Intriligator, D.S.: 1977, *Proc. 15th Int. Cosmic Ray Conf.* **11**, 225 – 229.
Iucci, N., Parisi, M., Storini, M., Villoresi, G.: 1979, *Nuovo Cimento B* **2**, 421 – 438.
Legrand, J.P., Simon, P.A.: 1981, *Solar Phys.* **70**, 173 – 195.
Lindblad, A., Lundstedt, H.: 1981, *Solar Phys.* **74**, 197 – 206.
Lindblad, B.A., Lundstedt, H.: 1983, *Solar Phys.* **88**, 377 – 382.
Lindblad, B.A., Lundstedt, H., Larsson, B.: 1989, *Solar Phys.* **120**, 145 – 152.
Maris, O., Maris, G.: 2005, *Adv. Space Res.* **35**, 2129 – 2140.
Mavromichalaki, H., Vassilaki, A.: 1998, *Solar Phys.* **183**, 181 – 200.
Mavromichalaki, H., Vassilaki, A., Marmatsouri, E.: 1988, *Solar Phys.* **115**, 345 – 365.
Mavromichalaki, H., Vassilaki, A., Tsagouri, I.: 1997, Joint European and National Astronomical Meeting (JENAM-97), Abstract 83.
Morley, S.K., Rouillard, A.P., Freeman, M.P.: 2009, *J. Atmos. Solar-Terr. Phys.* **71**, 1073 – 1081.
Parker, E.: 1959, *J. Geophys. Res.* **64**, 1675 – 1681.
Simon, P.A., Legrand, J.P.: 1992, *Solar Phys.* **141**, 391 – 410.